Stress and displacement analysis of powder packaging machine of capacity 2,600 pcs/hours

Stress and displacement analysis of powder packaging machine of capacity 2,600 pcs/hours

D H Al-Janan[1], Kriswanto[1], R Unggul[1], A Roziqin[1], R D Widodo[1], A Hangga[2], B Wiratama[1], B Wijayanto[3] and J Jamari[4]

[1]Department of Mechanical Engineering, Universitas Negeri Semarang, Gd E9 Kampus Sekaran Gunungpati, Semarang, Indonesia
[2]Department of Electrical Engineering, Universitas Negeri Semarang, Gd E11 Kampus Sekaran Gunungpati, Semarang, Indonesia
[3]Balai Pengembangan Teknologi Logam dan Kayu (BPTLK) Dinas Perindustrian dan Perdagangan Provinsi Jawa Tengah, Muktiharjo Lor, Semarang, Indonesia
[4]Department of Mechanical Engineering, University of Diponegoro, Jl. Prof. Sudharto Kampus UNDIP Tembalang, Semarang 50275, Indonesia

aljanan@mail.unnes.ac.id

Abstract. This study aims are to analyze stress and displacement using Finite Element Method (FEM) of the three components design of powder packaging machine. The safety factor (SF) is calculated to compare with the design acceptance criteria, more than two. The frame is made of ASTM A36 steel angle bar, while the camshaft and sealer sleeve of AISI 1018. Steel angle bar widths of 40x40 (mm) and 50x50 (mm) with a thickness of 3,4,5 (mm) use for the frame design variant. The diameters of the camshaft design variants are 0.75", 1", and 1.25". Then, the sealer sleeve variant utilizes thicknesses of 10, 12, and 14 (mm). Loading assumption during adverse operating conditions, such as when there is an obstacle or jam. Through the finite element method results, increasing the thickness of the frame also the sealer sleeve, and increasing the diameter of the camshaft, produced a decrease in the value of von mises stress and displacement. The safety factor for all variants of frame thickness was more than two, indicating that all designs were safe and acceptable. Nevertheless, there is one design failure on the camshaft and sealer sleeve because the SF value is less than two.

1. Introduction

Packaging is an integrated system for preserving and preparing items until they are ready to be supplied to end-users cost-effectively and efficiently. Furthermore, modern packaging other than product protection also functions as an indirect promotional tool and as a product brand image. Food products, instant drinks, and powdered drugs generally use flexible packaging in the form of bags or sachets. Flexible packaging materials can be aluminum foil, plastic film, cellophane, a metalized aluminum film, and paper with or without thermoplastic material. Therefore, packaging powdered products in the form of sachets require a machine that functions to form sachets, measure the net weight of the product, fill the product into the package, and close tightly. The packaging process using machines is carried out

automatically and hygienically using standard food-grade materials. Nevertheless, powder packaging machines are widely available in Indonesian and international markets have prices high enough to be reached by micro, small and medium scale enterprises (SMEs).

Designed a powder packaging machine with a minimum capacity of 2,600 pcs/hour that must meet the needs of small industries/SMEs at affordable prices. In addition, the component design needs to be cost-effective and still meets safety requirements when operated. Therefore, the strength of the component design is analyzed through the finite element method simulation to determine the stress, displacement, and safety factor values.

Research on the design and development of automatic powder packaging machines by applying simple pneumatic, mechanical, and electric systems more efficiently compared to other mechanic systems based on PLC or microcontroller [1]. This study streamlines the machine control system but does not analyze the machine's structural strength under extreme operating conditions.

The finite element (FE) approach is a numerical methodology used to approximation solutions to complex mathematical problems defined by differential equations [2]. Therefore, the finite Element Method (FEM) is a numerical and computer-based approach for resolving a wide range of real engineering issues [3]. As a result, it is critical to examine and investigate the strength and dependability of the engine, body, structure, or other components using FEM to enhance product stability, reliability, and safety [4]. FEM has evolved into an effective and widely used numerical approach for engineering analysis and design [5]. The study revealed that the smaller the size of the material, the smaller the value of the safety factor, and the cheaper the material costs when selecting the structural design of a machine based on FEM and assessment of material prices [6]. In addition, the structural strength of mechanical components is only tested under static loading not under thermal load. Several finite element method studies [2-12] establish the stress and deformation values of the design. It is quite expensive to test the developed product directly in the laboratory since the mechanical form of the product must be verified. The above literature uses the finite element method to predict stress and deformation under actual/planned loading conditions and evaluates using safety factor. The design of components subjected to extreme loads such as a jam needs to analyze for stress to obtain a safe design when it occurs. Not all of the studies above apply extreme loading conditions, even though the possibility of machine failure can occur and cause serious damage. Therefore, the purpose of the study is to analyze stress and displacement also determine the design of three components in the form of a frame, camshaft, and sealer sleeve that are safe in heavy operating conditions and terms of safety factors criteria of more than 2.

2. Design of Packaging Machine

The design of the packaging machine has a minimum production capacity of 2,600 pcs/hour with the functions of forming sachets, filling powder, and sealing. The packaging machine design (see Figure 1) includes (1) mainframe with dimensions of 900 mm long, 800 mm wide, and 1.7 m high; (2) the reservoir tube for powder products with a capacity of 5 kg made of STS 304 in the form of a 3 mm thick truncated cone; (3) panel boxes; (4) formers; (5) measuring plate; (6) plastic roll holder; (7) horizontal plastic sealer; (8) 0.5 HP electric motor; (9) gearbox ratio 1:30; (10) camshaft; (11) vertical plastic sealer; (12) 4 pieces of plastic pickup rollers; (13) stepper motors; (14) towing roller linkage chain; (15) flexible coupling; (16) 4 pieces of support wheels; (17) 20 mm UCFL bearings; and (18) bearing UCP 1 25.4mm.

3. Method

This study's method is a simulation of the finite element method to evaluate stress and displacement. This study uses the finite element method performed using Ansys software. Thermal analysis, structural analysis, computational fluid dynamics (CFD), harmonic analysis, modal analysis, transient dynamics, buckling, and many more issues can be simulate using Ansys. [7]

The finite element method is a numerical approach for solving partial differential equations and integral equations [8]. Ansys be used to conduct material strength analyses such as stress, displacement, and safety factor. Finite element equation generally uses the matrix in Equation (1).

$$[K]\{u\} = \{F\} \quad (1)$$

Where K is the (element) stiffness matrix, u is the (element nodal) displacement vector, and F is the (element nodal) force vector. Furthermore, k is the stiffness of the bar can also be calculated by Equation (2)

$$k=\frac{E\,A}{L} \tag{2}$$

Where E is the elastic modulus, A is the cross-sectional area, and L is the length,

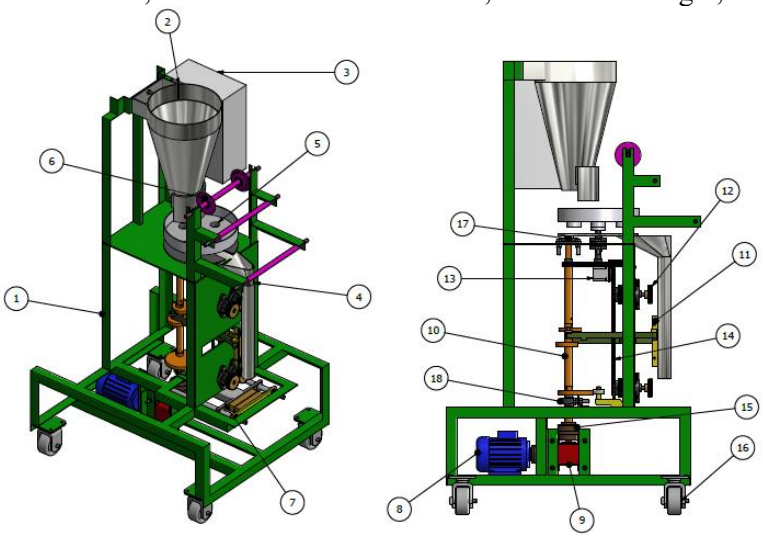

Figure 1. Packaging machine design

The major components of the packing machine are 18 in number (Figure 1), wherein three have studied in this simulation. The mainframe, camshaft, and vertical sealer sleeve were examined on the stress and displacement using finite element analysis. Meshing, material property selection, support selection, and loading are part of the preprocessing model [9]

3.1. Application of material properties

The frame material in the simulation is ASTM (American Standard Testing and Material) A36 steel angle, while the camshaft material is AISI (American Iron and Steel Institute) 1018 steel. Material mechanical properties are crucial input data for computational simulations [10]. Each element contains the appropriate material properties of each material. Computer-generated analysis can utilize material characteristics like Young's modulus and Poisson ratio to explain mechanical behavior, induced stress, or the connection between force and deformation for structural components [11].

Table 1. Material properties of ASTM A36 [13] and AISI 1018 [14]

Component	Material	ρ[kg/m^3]	v	σ_y[MPa]	E[GPa]
Frame	ASTM A36	7850	0.26	245	200
Camshaft	AISI 1018	7860	0.29	370	205
Sealer sleeve	AISI 1018	7860	0.29	370	205

Where ρ is the density, v is the poisson ratio, σ_y is the yield strength of the material, and E is the modulus of elasticity.

3.2. Mesh settings

Table 2 shows the mesh size of each component and the kind of mesh utilized, which is a tetrahedron. Furthermore, to ensure that the mesh reaches high quality, a convergence test is performed. If the difference in stress results between before and after addition meshes was minimal, increasing the number of elements halted.

Table 2. Mesh size of packaging machine components

Component	***Sizes***		
	Absolute *[mm]*	***Number of Element***	***Nodes***
Frame	*10*	*166,248*	*341,681*
Camshaft	*3*	*42,890*	*78,042*
Sealer sleeve	*5*	*3,394*	*6,684*

3.3. Loading and boundary conditions

3.3.1. Load on main frame. The packing machine frame made from ASTM A36 steel of 17.5 meters length, which needs 2.95 times the bar of angled steel. The frame design and loading of a powder packaging machine as shown in Figure 2. The loads on the mainframe calculate using Equation 3-8. Table 3 also shows the load calculation results for the frame.

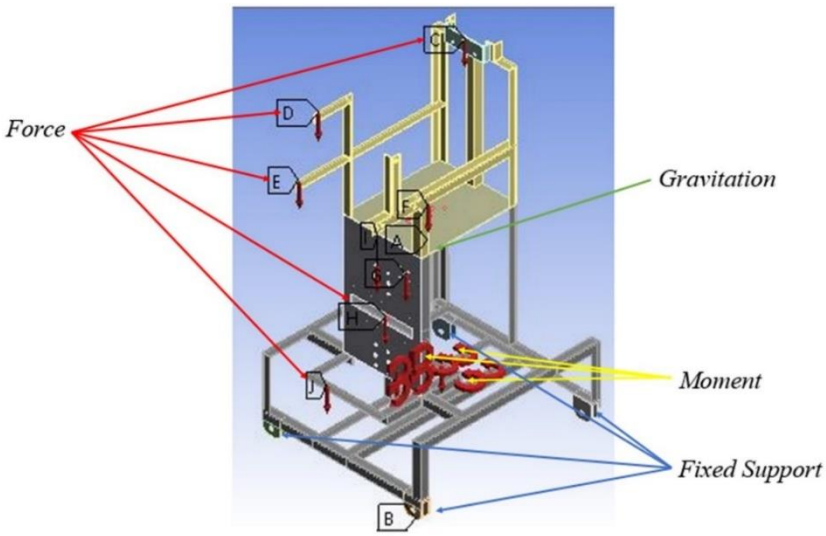

Figure 2. Loading on the frame

$$W = m.g \tag{3}$$

$$W_{ra} = W_t + W_{rp} + W_{pr} + W_{dp} + W_b \tag{4}$$

$$W_{rt} = W_{ro} + W_{ms} + W_{ls} + W_{sb} + W_b \tag{5}$$

$$W_{rb} = W_{pc} + W_m + W_{gb} + W_{cf} \tag{6}$$

$$W_{cf} = W_{cf1} + W_{cf2} \tag{7}$$

$$\tau = F.r \tag{8}$$

Table 3. Load data applied to frame components

	W_{gb} [N]	W_{ro} [N]	W_{ms} [N]	W_{rp} [N]	W_{ls} [N]	W_{sb} [N]	W_t [N]	W_{pr} [N]
Value	98	31.56	10.78	29.4	28.91	33.22	186.2	29.4
	W_{dp} [N]	W_b [N]	W_{pc} [N]	W_m [N]	W_{cf1} [N]	W_{cf2} [N]	τ_b [Nm]	g [m/s^2]
Value	18.62	38.22	52.92	166.6	11.76	16.66	9.8	9.8

Where W_{gb} is the gearbox load, W_{ro} is the roller load, W_{ms} is the stepper motor load, W_{rp} is the plastic roller load, W_{ls} sealer sleeve load, W_{sb} is the horizontal sealer load, W_t is the tube load, W_{pr} is the measuring disc load, W_{dp} is the disc mount load, W_b is the bearing load, W_{pc} is the camshaft load, W_m is the electric motor load, W_{cf1} is the flexible coupling load 60, W_{cf2} is the flexible coupling load 80, $\boldsymbol{\tau_b}$ is the bolt moment.

3.3.2. Load on Camshaft. The camshaft is made of AISI 1018 while the mechanical properties show in Table 1. The load applied to the camshaft is calculated using Equation 9-12 and the result is shown in Table 4. Figure 3 illustrates the design of the camshaft. The loading and boundary conditions to the camshaft as shown in Figure 5, wherein it consists of fixed supports located at both ends of the shaft and then the moment of force on each cam. In this study, the load assumption applied to the camshaft constrained (jammed) also received a heavy load.

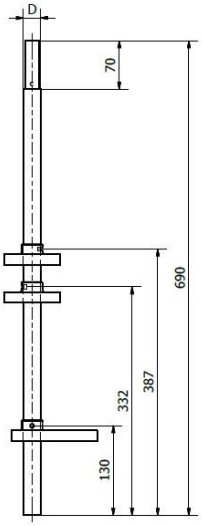

Figure 3. Cam shaft design

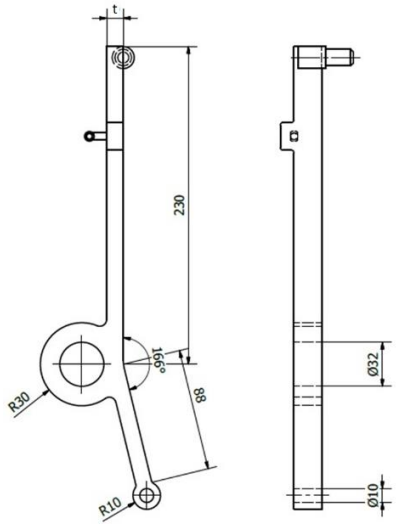

Figure 4. Sealer sleeve design

$$\tau_{gx} = \frac{60\ x\ P}{2.\pi.ns} \tag{9}$$

$$n_s = \frac{d_1}{d_2} n_m \tag{10}$$

$$F_{cam} = \frac{\tau_{gx}}{r} \tag{11}$$

$$F_{ss} = F_{cam}.Cos\ \theta \tag{12}$$

Where τ_{gx} is the gearbox torque, P is the power of electro motor, n_s is the rotational speed of shaft, n_m is the rotational speed of motor, $\frac{d_1}{d_2}$ is the gearbox ratio (1:30), F_{cam} is the force of camshaft, F_{ss} is the force to the sealer sleeve, and θ is the working angle of the sealer sleeve at 5.19°.

Table 4. The Camshaft loads

P [Watt]	n_m **[rpm]**	n_s**[rpm]**	τ_{gx}**[Nm]**	F_{cam}**[N]**
373	1400	46.67	76.37	332.04

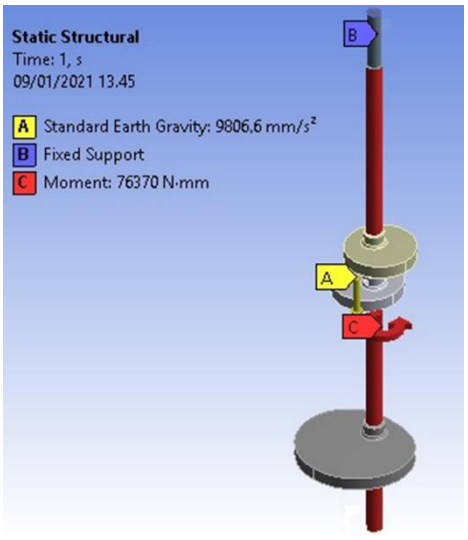

Figure 5. Load on the camshaft

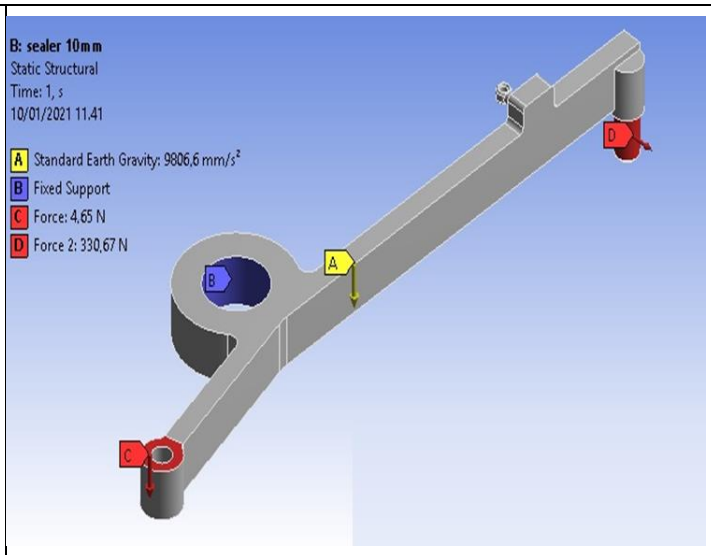

Figure 6. Load on sealer sleeve

3.3.3. Load on sealer sleeve. Table 5 displays the load data applied in the sealer sleeve, whereas Figure 4 depicts the sealer sleeve design. The sealer sleeve constrained fixed support, while the loading in cam force and weight of sealer house is shown in Figure 6. The thermal load measured by direct measurement of the sealer sleeve via thermostat, which then temperature data was applied as shown in Figure 7. The load assuming the sealer sleeve is constrained (jammed) or gets a heavy load.

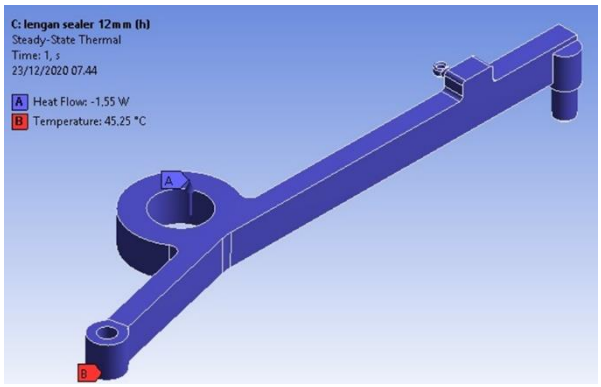

Figure 7. Thermal load on sealer sleeve

Table 5. Load and thermal data on sealer sleeve

	F_{sealer} [N]	g [m\s^2]	T [^{0}C]	F_{ss} [N]	*Heat Flow* 1 [W]	*Heat Flow* 2 [W]	*Heat Flow* 3 [W]
Value	4.65	9.8	45.25	330.67	1.29	1.55	1.81

Where F_{sealer} sealer housing load, g is the gravity, and T is the temperatur sealer.

3.4. Model validation

The von mises stress generated from the finite element method is compared with the calculated bending stress on the frame. Before calculated the bending, the moment and force action calculate according to the free body diagram in Figure 8.

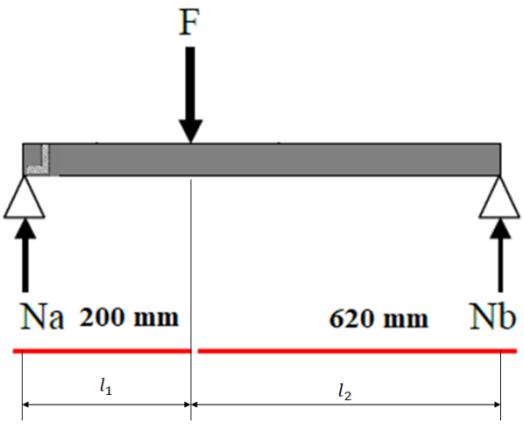

Figure 8. Free body diagram of bending load on electro motor holder

Forces and moments according to FBD calculated using Equation (13-16). Equation (17) use for calculating the moment of inertia using and then Equation 18 used for calculating the bending stress.

$$\sum Fx = 0;\ \sum Fx = 0; \sum M_{Na} = 0 \quad (13)$$

$$\text{Na} + \text{Nb} - \text{F} = 0 \quad (14)$$

$$M_{Na} = Na.l_0 + F.l_1 - Nb.l_2 \quad (15)$$

$$M_{ba} = F\ .\ l \quad (16)$$

$$I_1 = \frac{B_1.{H_1}^3}{12};\ I_2 = \frac{B_2.{H_2}^3}{12};\ \text{I}=I_1 + I_2 \quad (17)$$

$$\sigma_b = \frac{M_{ba}\ c}{I} \quad (18)$$

Where σ_b is the flexural stress, M_{ba} is the maximum bending moment, c is the distance from the base to neutral axis, I is the moment of inertia exerted on the bending axis, f is load of electromotor on structural, l is the length of structural, B and H is the dimension of angle bar, Na is the reaction at support A, and N_b is the reaction at support B.

4. Results and Discussion

4.1. Model validation

The model validation obtains by comparing the stress analysis by FEM with the bending stress on the electromotor mount. Further, the maximum stress value is colored in red area in the FEM, which is 16.49 MPa (Figure 9). Nevertheless, the bending stress value presented in Table 6.

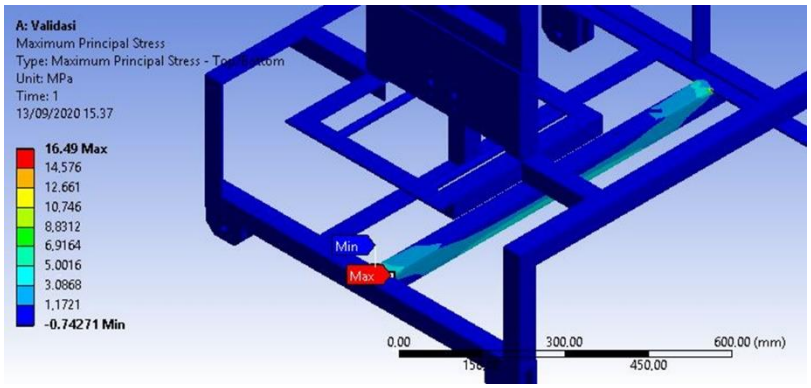

Figure 9. Maximum stress of electromotor holder

Table 6. Load and bending stress of model

F [n]	L [mm]	Na [N]	Nb [N]	M_{ba} [Nmm]	M_{Na} [Nmm]	I_1 [mm^4]	I_2 [mm4]	I [mm4]	C [mm]	σ_b [MPa]
173.14	820	117.2	55.85	14,1974.8	0.38	12,663.25	90	12753.25	1.5	16.69

The calculated bending stress is 16.69 MPa while the simulated is 16.49 MPa, so the difference between the two methods is 1.1%. Therefore, the difference in stress results between the two methods is closer, so the finite element method uses to analyze stress and displacement.

4.2. Analysis of stresses and displacements in frame components.

Table 7 shows the von mises stress (σ_{von}) and displacement (δ) from the static analysis using the finite element method, as well as the computation of the factor of safety (*Sf*) for changes in frame size. The frame is built of ASTM A36 angle bar in the following sizes: 40x40x3, 40x40x4, 40x40x5(mm). The von Mises stress in ductile materials provides an appropriate scalar measure of the complex stress field [15].

The safety factor is the result of comparing the maximum stress simulation results to the yield strength value. The analysis factor of safety that yields a similar to the original but does not exceed the yield strength value is chosen [16], Furthermore, the safety factor takes to account a semi-probabilistic safety format based on boundary state with a partial safety factor applied to the material's load and strength [17]. Equation 19 used to compute the value of the safety factor of the packing machine components. For the design of machine parts that sustain dynamic loads with an average probability value for all design data, the safety factor of packing machine components ranges from 2.0 to 2.5 [18].

$$Sf = \frac{\sigma_{yield}}{\sigma_{design}} \tag{19}$$

Table 7. Stress, displacement, and safety factor of variations in frame size

Variations	**Material size [mm]**	σ_{von} **[Mpa]**	δ **[mm]**	***Sf***
Frame1	40x40x3	57.10	0.33	4.37
Frame 2	40x40x4	54.34	0.3	4.6
Frame3	40x40x5	42.19	0.27	5.92

Figure 10 indicates that the maximum von mises stress is 57.10 MPa in frame 1 and the lowest stress is 42.19 MPa in frame 3. According to the FEM results, the thicker the frame on the steel angle bar, the lower the von mises stress. The maximum von mises stress is found on the red region (see Figure 11), which is on the gearbox holder, which receives moments and loads from the gearbox. Stress analysis conducts to ensure that the design will perform as planned in a given loading environment [19].

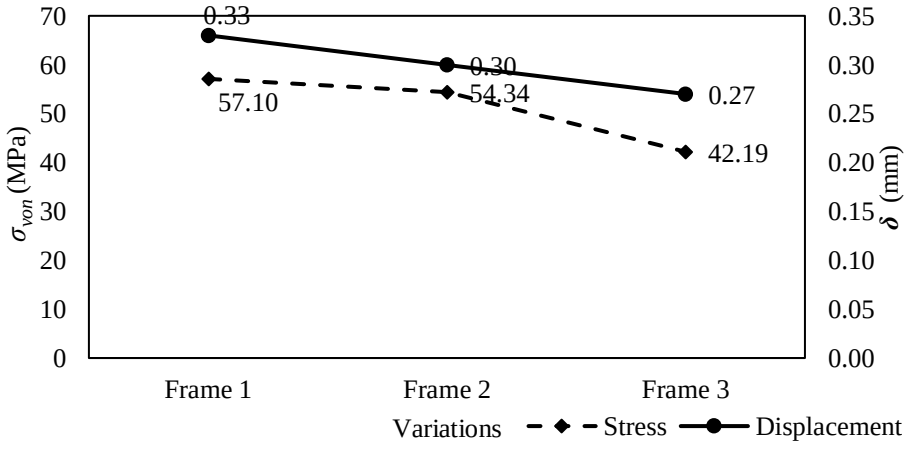

Figure 10. Graph of von mises stress and displacement on the frame

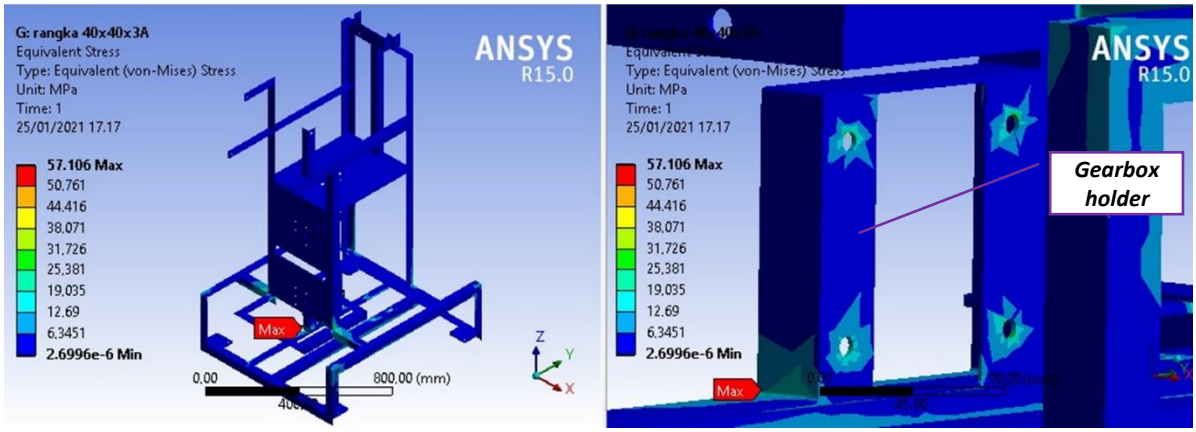

Figure 11. Von mises stress on frame 1

The displacement value of the simulation results reveals that frame 3 has the least displacement value of 0.27 mm and frame 1 has the highest displacement of 0.33 mm. Furthermore, the displacement values also decreased from the addition of the frame thickness (see Figure 10). This is similar to the results of von mises stress analysis. Each frame variation has a displacement value that is less than 0.5mm. As a result, the displacement that happens in the red region, namely the reservoir tube holder (Figure 12), has no effect on the machine's critical components, and so the displacement is not a matter. The lowest safety factor for frame components was 4.37 on frame 1 and the highest was 5.92 on frame 3. Furthermore, when compared to the safety factor criteria in this study, it must be larger than 2, and then all variants of the frame are regarded safe.

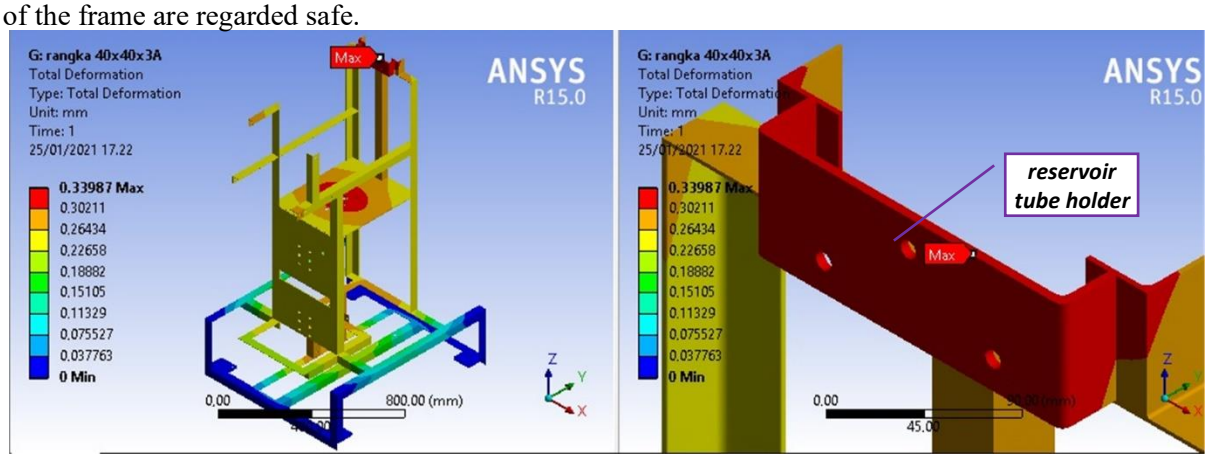

Figure 12. Deformation on frame 1

4.3. Analysis of stresses and displacements in camshaft

The camshaft is made of AISI 1018 and available in three sizes: 0.75", 1", and 1.25" subjected to static and thermal loads. Furthermore, Table 8 displays the von mises stress (σ_{von}) and displacement (δ) generated by the finite element method, as well as the factor of safety (Sf) due to camshaft size changes.

Table 8. Stress, displacement, and safety factor of variations on camshaft

Variations	Diameter (mm)	σ_{von} (MPa)	δ (mm)	*Sf*
Camshaft 1	0.75	245.68	0.39	1.51
Camshaft 2	1	112.85	0.13	3.28
Camshaft 3	1.25	66.39	0.05	5.57

Camshaft of 1 is the highest von mises stress (245.68 MPa), while camshaft 3 has the lowest (66.39 MPa). Figure 13 indicates the influence of a large shaft diameter on the resultant stress, showing that the larger the shaft diameter, the lower the von mises stress. Furthermore, the similar circumstance in displacement, where there is a decrease in displacement value due to an increase in shaft diameter.

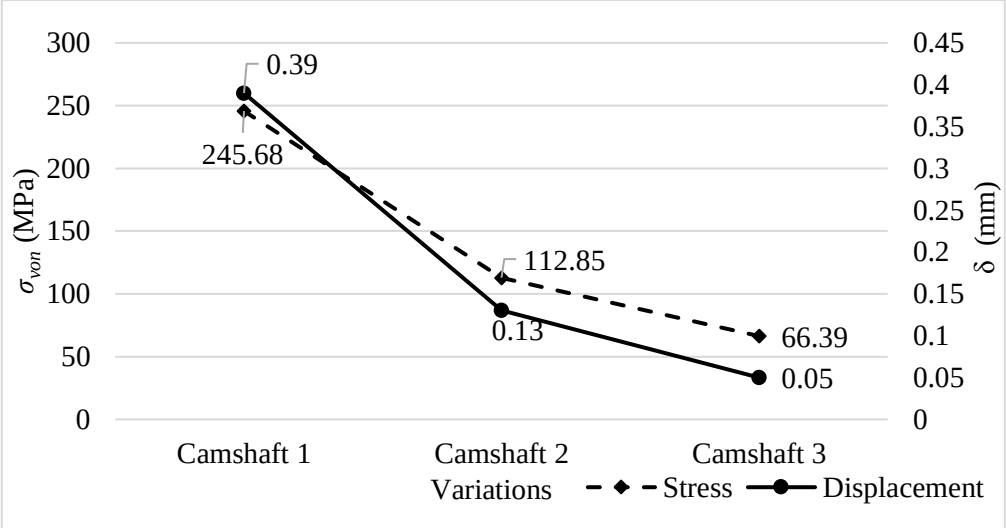

Figure 13. Graph of von mises stress and displacement on the camshaft

The simulation's highest displacement value (0.39mm) is in camshaft 1, while the lowest deformation (0.05mm) is in camshaft 3. Furthermore, the cam (red region) has the most deformation, as illustrated in Figure 15. The camshaft 3 has the highest safety factor of 5.57, while camshaft 1 has the lowest safety factor of 1.51. Furthermore, only camshafts 2 and 3 have a safety factor greater than 2, and camshaft of 1 is declared a failure. The failed design from the analyzed is not recommended for application to the manufacture of packaging machine components. So that one of the advantages of utilizing FEM to stress analysis of the manufacturing process and product development is reduced production costs [20].

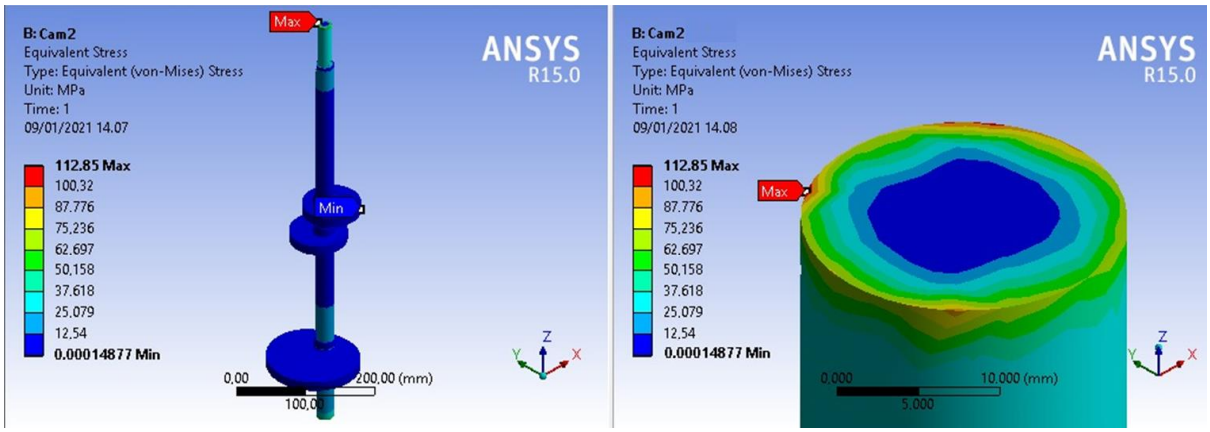

Figure 14. Von mises stress on camshaft 2

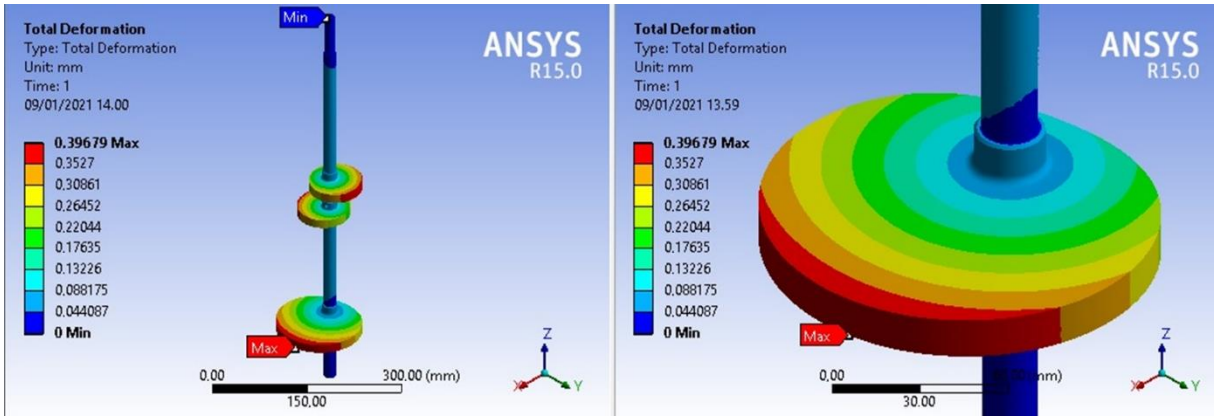

Figure 15. Displacement on camshaft 1

4.4. Analysis of stresses and displacements in sealer sleeve

Table 9 indicates sealer sleeve 1 produces the highest von Mises stress (201.81 MPa) while sealer sleeve 3 produces the lowest (120.97 MPa). The stress and displacement results of the sealer sleeve are similar to the frame and camshaft, which reduces as material size increases.

Table 9. Stress, displacement, and safety factor of variations on sealer sleeve

Variations	Thickness, *t* (mm)	σ_{von} (MPa)	δ (mm)	*Sf*
Sealer sleeve 1	10	201.81	2.8	1.83
Sealer sleeve 2	12	156.53	1.6	2.36
Sealer sleeve 3	14	120.97	1.04	3.06

Figure 17 depicts the highest von mises stresses in the red area. Adding thickness dimensions to the design, it will increase stiffness referring to Equation (2). These results are similar with the study of increased component size can reduce stress and displacement [5]. The displacement value of the sealer sleeve has higher than the frame or camshaft, with the lowest value being 1.04 mm and the maximum being 2.8mm. The stresses and deformations of the sealer sleeve effect by the load that is assumed to be in a pinched sleeve condition (in static condition), driven by a cam, and thermal load subjected.

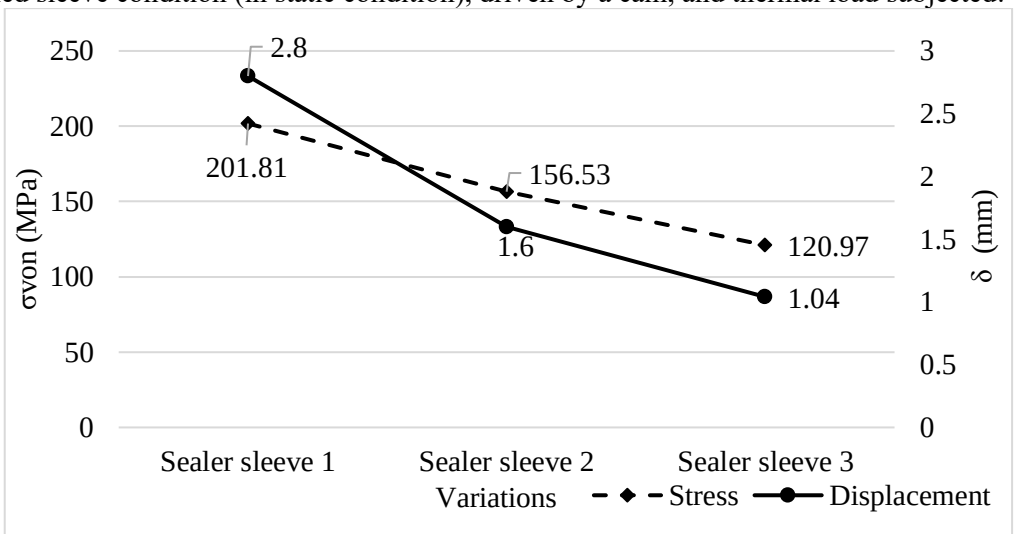

Figure 16. Graph of von mises stress and displacement on the sealer sleeve

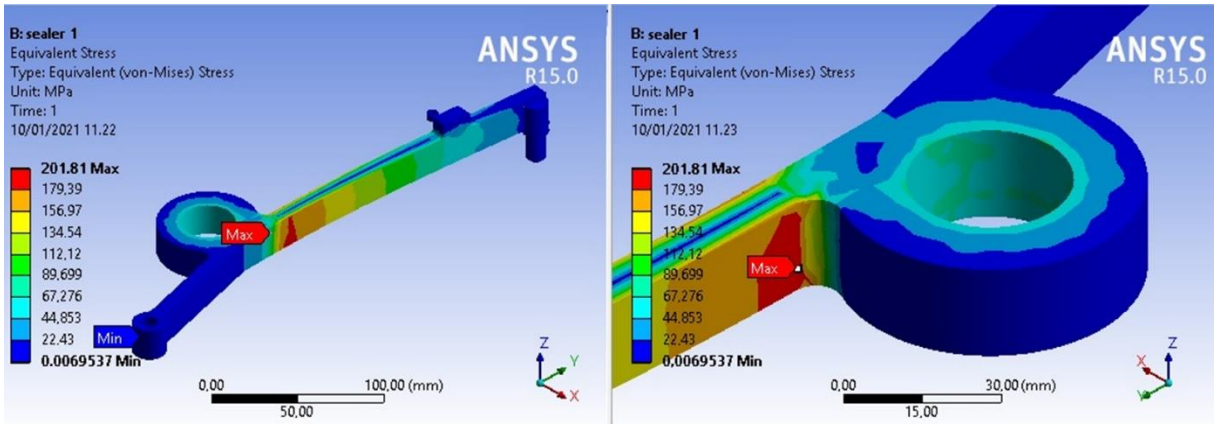

Figure 17. Von mises stress of the sealer sleeve 1

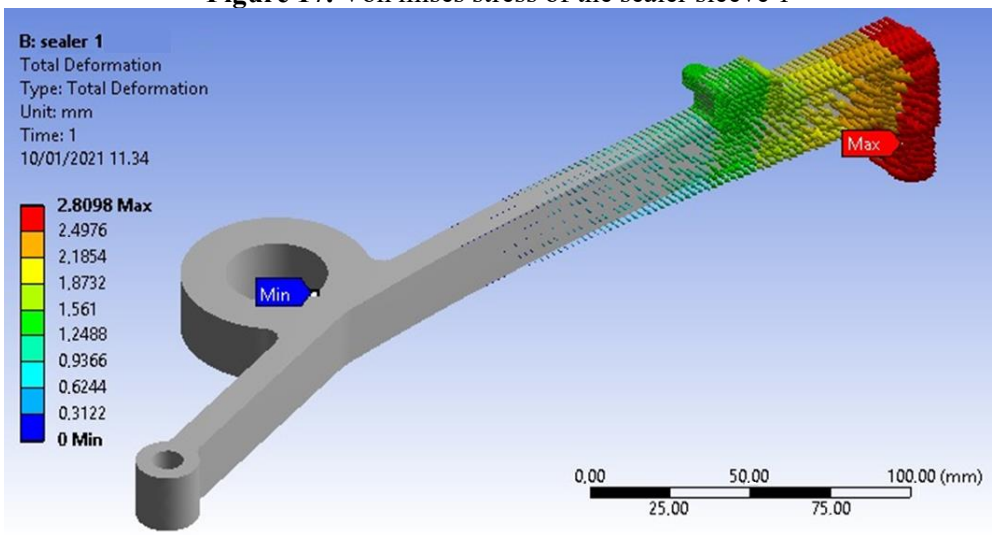

Figure 18. Deformation of the sealer sleeve 1

Stress analysis on the sealer sleeve design is utilized to ensure that the design does not fail when encountered impediments (jams) or excessive application. The highest displacement of the sealer sleeve as a red vector is shown in Figure 18. Based on the safety factor criterion, which must be more than two, the design of sealer sleeve 1 with SF 1,83 is deemed inadequate. Furthermore, the design variations of 2 and 3 are declared safe

5. Conclusions

Powder packing machine components are simulated under heavy working loads and required to meet a safety factor of more than two. The difference of the stress result between the FEM simulation and calculation is 1.1%, so the FEM can be used to analyze stress and displacement. Furthermore, the simulation findings reveal that as material size increased, the von mises stress and displacement of the three components, namely the frame, camshaft, and sealing sleeve, reduced. In general, increasing the size or thickness increases the value of the cross-sectional area, therefore increasing the stiffness of the design. Furthermore, the component evaluation based on the safety factor criteria found that all variations of the frame design were declared safe wherein the SF value exceeded 2. While in the camshaft and sealer sleeve designs, each design there was one design that failed, namely camshaft of 1 (0.75 " diameter) with SF 1.31 and sealer sleeve of 1 (thick 10mm) with SF 1.83. The frame and camshaft variations have a small displacement below 0.4mm, while the sealer sleeve design has a displacement value of more than 1 mm and a maximum of 2.8 mm on the sealer sleeve 1. Further, since variation 1 of the sealer sleeve does not fulfill the safety factor, the highest displacement occurs in the sealer sleeve of

2 (1.6mm).

References

[1] Saraf M R, Rulwale V V, Kulkarni V V and Kulkarni S M 2016 *International Journal of Current Engineering and Technology* **4** 420-424
[2] Baccouch M 2020 *Finite Element Methods and Their Applications* (London: IntechOpen)
[3] Anderson R, Andrej J, Barker A, Bramwell J, Cerveny J S, Dobrev V, Dudouit Y, Fisher A, Kolev T, Pazner W, Stowell M, Tomov V, Akkerman I, Dahm J, Medina D and Zampini S 2020 *Computers and Mathematics with Applications* **81** 42-74
[4] Chen Y 2020 *IOP Conference Series: Material Science and Engineering*
[5] Li L, Shen T and Li Y K 2017 A *Journal of Manipulative and Physiological Therapeutics* **40** 580-586
[6] Kriswanto, Supraptono, Roziqin A, Hasyim F, Saputro D D and Wijayanto B 2021 *IOP Conf. Series: Earth and Environmental Science* **700** 012004
[7] Vaishnav N and Dubey S 2019 *Journal of Modern Engineering & Management Research* **7** 11-19
[8] Chandru B T and Suresh P M 2017 *Materials Today Proceedings* **4** 11237-44
[9] Babu A V H and Prasad B D 2019 *Materials Today Proceedings* **16** 295-301
[10] Moreira T M M, Godefroid L B, Faria G L D and Silveira R A D M 2019 *Engineering Failure Analysis* **106** 1-12
[11] Lakshmi R D, Abraham A, Sekar V and Hariharan A 2015 *Tanta Dental Journal* **12** 56-64
[12] Moreno M F, Bertolino G and Yawny A 2016 *Materials and Design* **95** 623–63
[13] Anonymous 2005 *Standart Specification for Carbon Structural Steel* (West Conshohocken: ASTM International)
[14] Anonymous AISI 1018 Steel, cold drawn datasheet http://www.matweb.com/search/datasheet_print.aspx?matguid=3a9cc570fbb24d119f08db22a53e2421
[15] Fuente E D L 2009 *Computers and Structures* **87** 1253–62
[16] Noor M A M, Rashid H, Mahyuddin W M F W, Azlan M A M and Mahmud J 2012 *Proceeding Engineering* **41** 995-1001
[17] Cugat V, Cavalaro S H P, Bairan J M and Fuente A D L 2020 *Tunnelling and Underground Space Technology* **103** 1-8
[18] Mott R L 1985 *Machine Element in Mechanical Design* (Princeton: Merril Publishing Company)
[19] Aryadi W, Kriswanto, Roziqin A and Jamari J 2021 *IOP Conf. Series: Earth and Environmental Science* **700** 012006
[20] Roziqin A, Kriswanto and Aryadi W 2021 *IOP Conf. Series: Earth and Environmental* Science **700**012008